Electronic Supplementary Material (ESI) for RSC Advances.

Supporting Information

White light emission by controlled mixing of carbon dot and rhodamine B for applications in optical thermometry and selective Fe^{3+} detection

*Sonam Mandani, Bhagwati Sharma, Deepa Dey and Tridib K. Sarma**

Discipline of Chemistry, Indian Institute of Technology Indore, Simrol Campus, Khandwa Road, Indore– 453552, India

Email: tridib@iiti.ac.in

1. Materials and Methods:

1.0 Materials:

β- carotene was purchased from Sisco Research Laboratories, India. Rhodamine B was obtained from Sigma and the salts namely copper nitrate, zinc nitrate, ferric nitrate, cadmium nitrate, nickel chloride, potassium chloride, sodium chloride, mercuric chloride, magnesium chloride and calcium chloride were purchased from Merck, India. All the chemicals were used as received and MilliQ water was used throughout the experiments.

1.1 Synthesis of C-dots:

In a typical procedure, β-carotene at a concentration of 0.5 mg mL−1 was dispersed in water in a sealed glass tube which was subjected to microwave irradiation at power 150 watts and temperature 150 °C for 45 minutes. This resulted in a pale yellow dispersion of luminescent C-dots. The solution was filtered through a Whatman filter paper to remove any insoluble part before using for further experiments.

1.2 Preparation of white light emitting composite:

A 2 x 10^{-4} M solution of rhodamine B was prepared and aliquots were added to 2 mL of C-dot dispersion (0.45 mg/ mL) for fluorimetric studies. The white light emitting composite was formed at the final RhB concentration of 20 μM.

1.3 : Assay of metal ions:

2 mL C-dot-RhB mixture was titrated with aliquot of 5 μL of 1 mM solution of different metal salts. The solutions were equilibrated for 2 mins at room temperature before recording the spectra.

1.4 Instrumentation:

Microwave irradiation experiments were performed in a focused microwave CEM discover reactor. A Varian Cary 100 Bio spectrophotometer was used for UV-visible measurements. Emission spectra were recorded using a fluoromax-4p fluorometer from Horiba (Model: FM-100). A FEI Technai G2, F30 microscope operating on voltage 300 kV and a JEOL JEM-2100 microscope operating on voltage of 200kv were used to obtain the transmission electron microscopy (TEM) images. The time resolved fluorescence studies were performed on Horiba Yvon (model: Fluorocube-01-NL), a nanosecond time correlated single photon counting (TCSPC) system. The dynamic light scattering (DLS) and zeta potential studies were done on a Micromeritics Nanoplus 3 instrument.

1.5 Time Resolved Fluorescence measurements:

For the time resolved studies, we used a picosecond time correlated single photon counting (TCSPC) system from Horiba Yovin (Model: Fluorocube-01-NL). The samples were excited at 375/405 nm using a picosecond diode laser (model: Pico Brite-375L). The repetition rate was 5 MHz. The signals were collected at magic angle (54.70^o) polarization using a photomultiplier tube (TBX-07C) as the detector, which has a dark count of less than 20 cps. The instrument response function of our setup is 140 ps. The data analysis was done using IBH DAS (version 6) decay analysis software. The fluorescence decay was described as a sum of exponential functions:

$$D(t) = \sum_{i=1}^{n} a_i \exp\left(\frac{-t}{\tau_i}\right)$$

Where $D(t)$ is the normalized fluorescence decay. τ_i are the fluorescence lifetimes of various fluorescent components and a_i are the normalized pre-exponential factors. The amplitude weighted lifetime is given by:

$$\langle \tau \rangle = \sum_{i=1}^{n} a_i \tau_i$$

The quality of the fit was judged by reduced Chi square (χ^2) values and the corresponding residual distribution. To obtain the best fitting in all of the cases, χ^2 was kept near to unity.

1.6 Photostability measurements:

For photostability test, the samples were irradiated under a low pressure UV lamp (wavelength 356 nm and power 6 W) obtained from Scientific Aids and Instrument Corporation, India . PL imaging and decay of an individual C-dot was obtained using a custom-made microscope setup based on an inverted fluorescence microscope (Nikon, Eclipse Ti-U) coupled with a back-illuminated electron-multiplying charge-coupled device (EM-CCD) camera (Andor, iXon X3 897). An air-cooled argon ion laser (Melles Griot, 400-A03) was used as a source of excitation light. A collimated laser beam of 457 nm wavelength was passed through a beam expander (Holmarc, India) and a neutral density filter (Sigma Koki, Japan). The beam was then directed toward the center of the

back aperture of an oil immersion objective (Apo TIRF, Nikon, 100×, NA = 1.49) parallel to the objective axis and subsequently focused on its back focal plane. The PL signal was filtered by a 505 nm dichroic mirror and a 520 nm long-pass filter. Finally, the images were captured by the back illuminated EM-CCD camera at a frame rate of 200 ms with no binning. The images were analyzed with ImageJ (version 1.47v) by the National Institutes of Health (NIH).

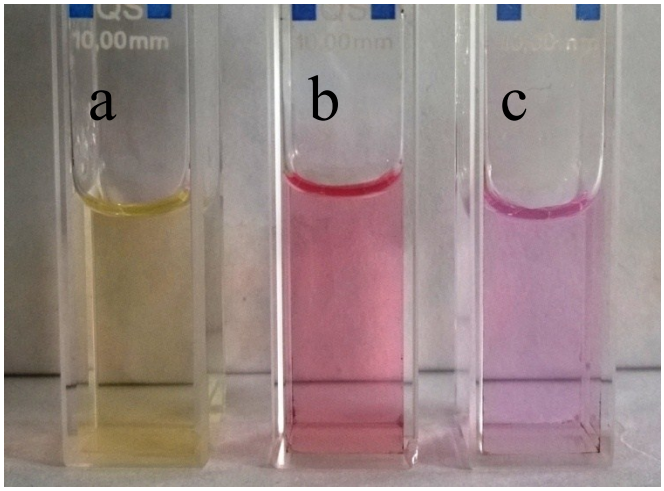

Figure S1.Digital images of (a) C-dots from β-carotene, (b) C-dot-RhB composite and (c) RhB solution, all in water.

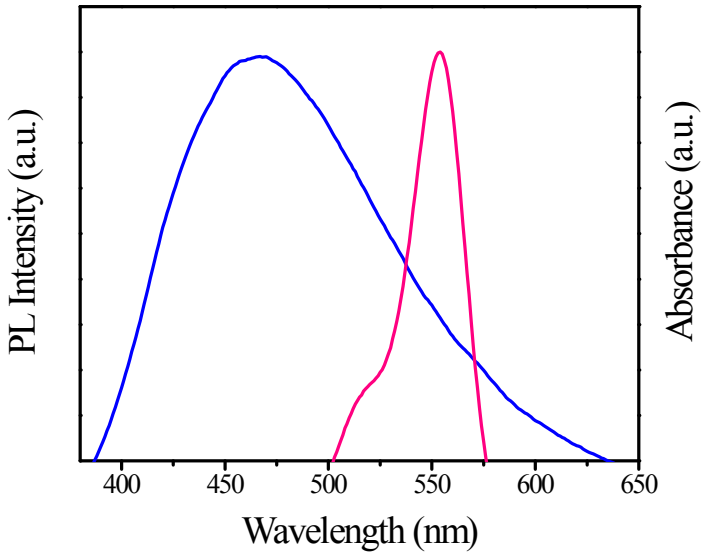

Figure S2. Spectral overlap of fluorescence emission of C-dots (blue) when excited at λ_{ex} = 365 nm and absorption spectra of RhB (pink).

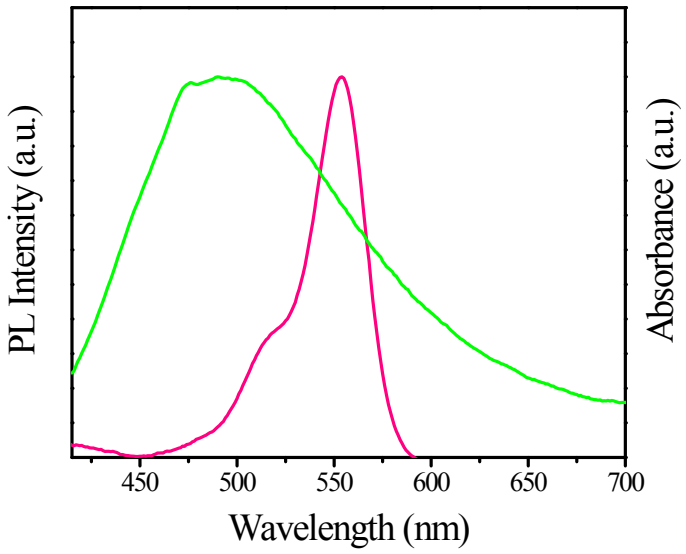

Figure S3. Spectral overlap of fluorescence emission of C-dots (green) when excited at λ_{ex} = 405 nm and absorption spectra of RhB (pink).

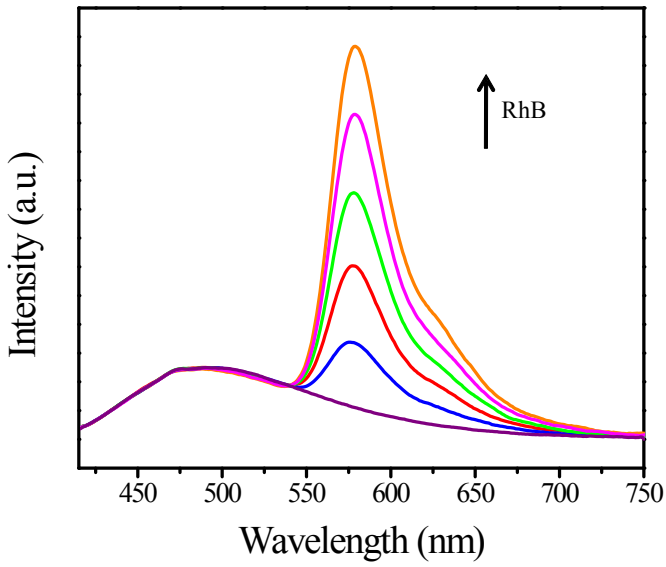

Figure S4. Fluorescence spectrum of C-dots upon increasing concentration of RhB recorded at λ_{ex} = 405 nm

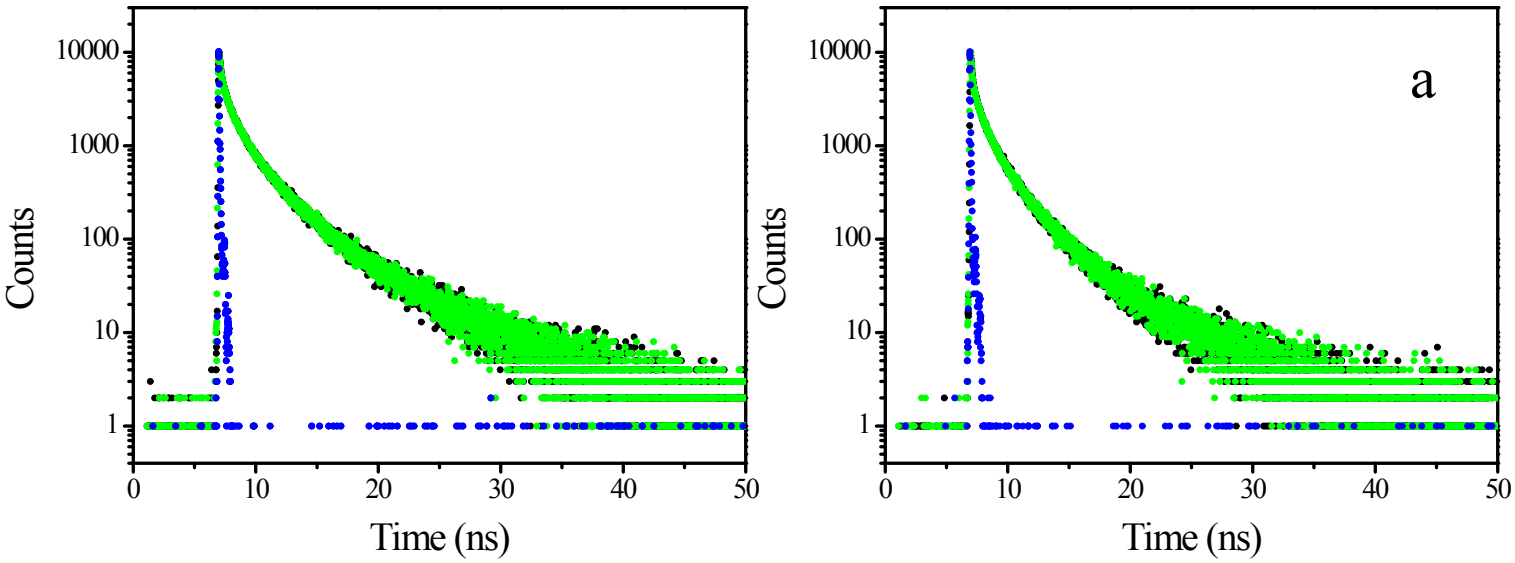

Figure S5. Lifetime decay curves of only C-dots (black) and C-dots in C-dot-RhB composite (green) excited at (a) 375 nm and (b) 405 nm respectively. Blue plot denotes the instrument response function.

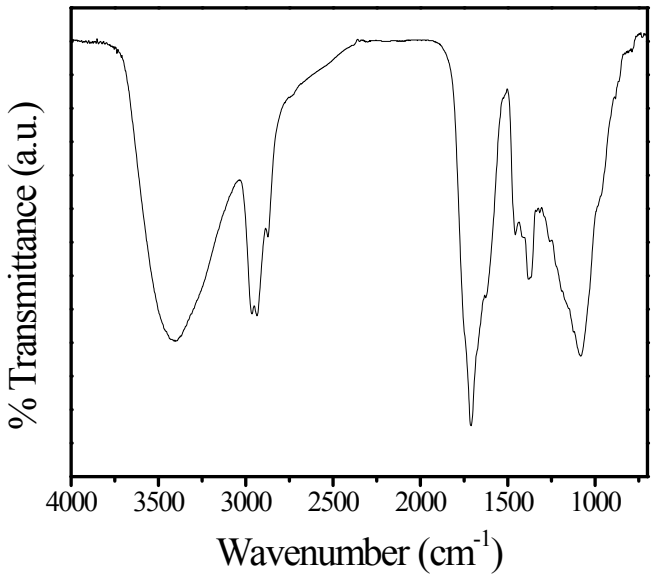

Figure S6. FTIR spectra of C-dots illustrating the characteristic features including stretching vibrational peak of O-H at 3400 cm^{-1}, the C=O stretching vibrational peak at 1710 $cm^{-1}$and the C-O stretching vibration at 1080 cm^{-1}.

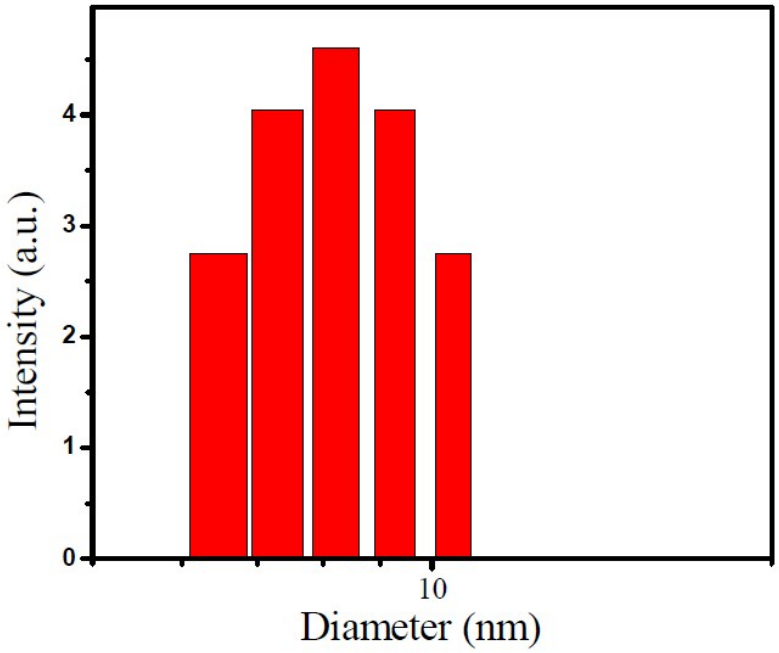

Figure S7. Dynamic light scattering analysis of C-dots. The average particle size was found to be 8. 5 ± 3.4 nm.

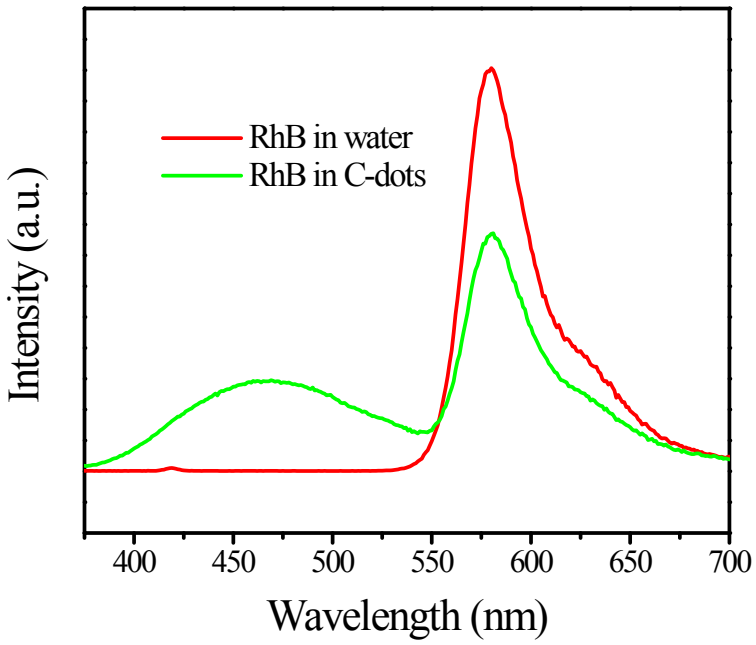

Figure S8. Fluorescence emission of RhB in presence and absence of C-dots in aqueous medium.

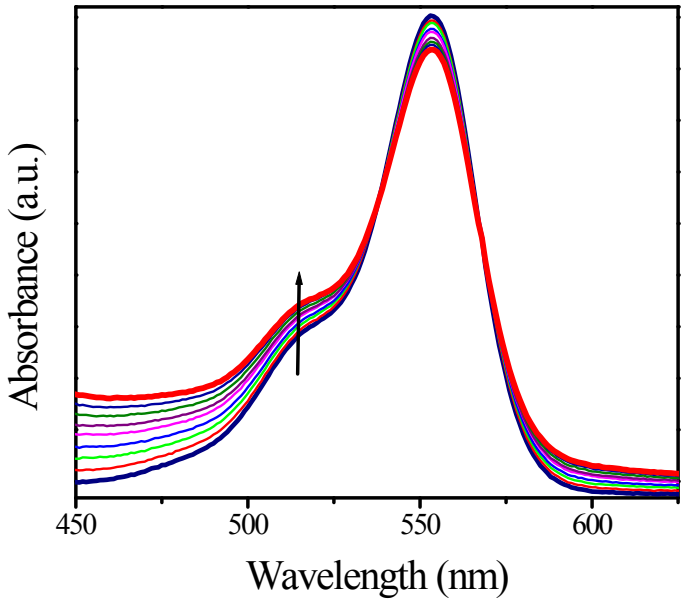

Figure S9. UV-Visible spectra of RhB upon increasing concentration of C-dots suggesting the formation of H-type aggregates.

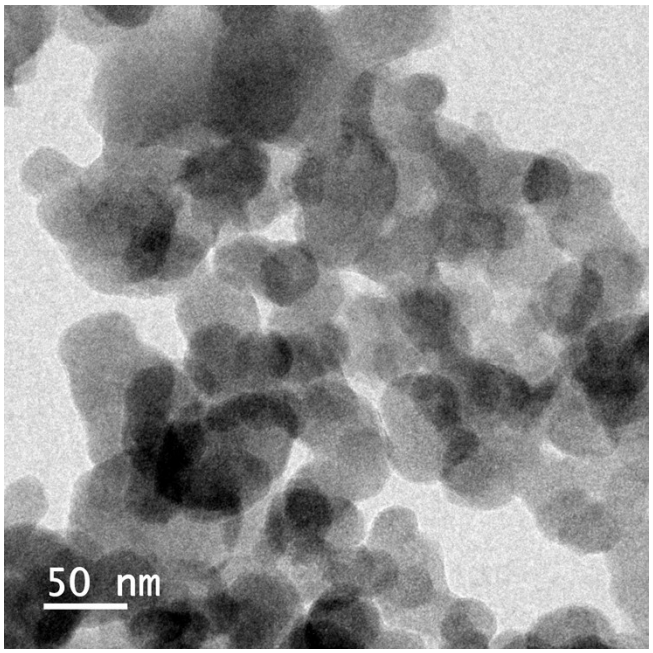

Figure S10. TEM image of C-dot-RhB composite showing the formation of agglomerated nanocomposite.

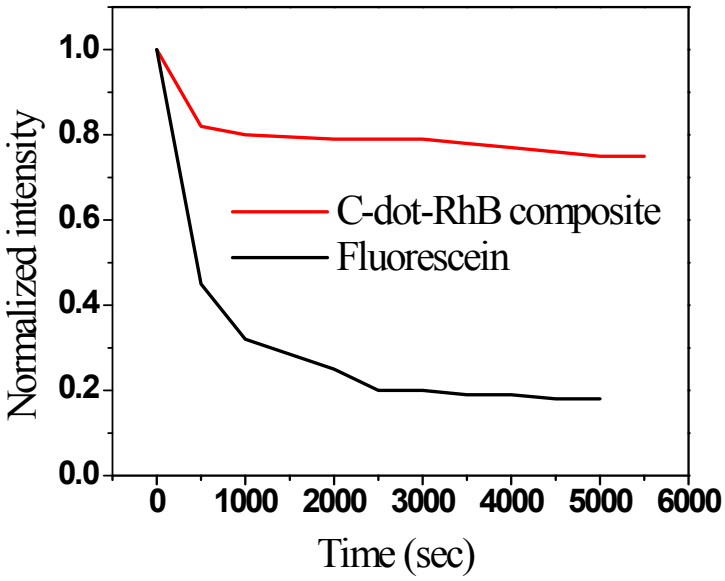

Figure S11. Photobleaching properties of C-dot-RhB composite and fluorescein.

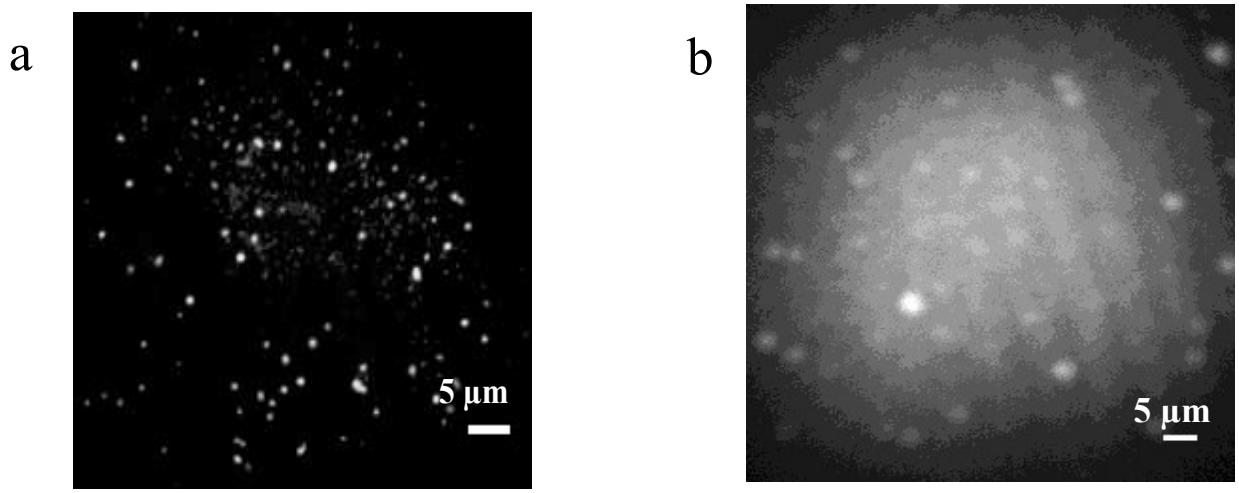

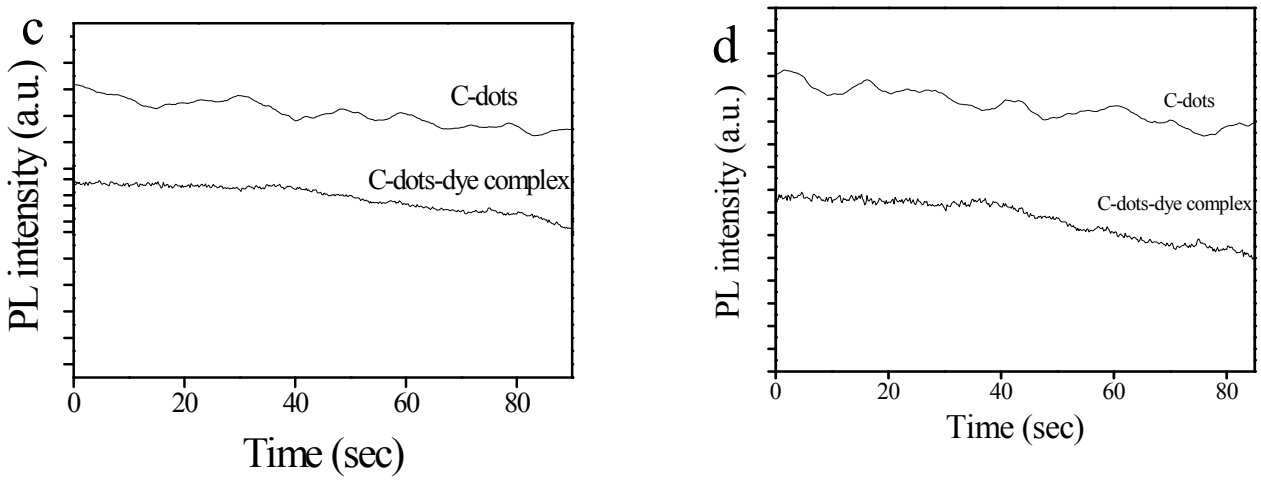

Figure S12. PL image of (a) C-dots and (b) C-dot-RhB composite,

(c) and (d) PL time traces of two luminescent spots of C-dot and C-dot-RhB composite.

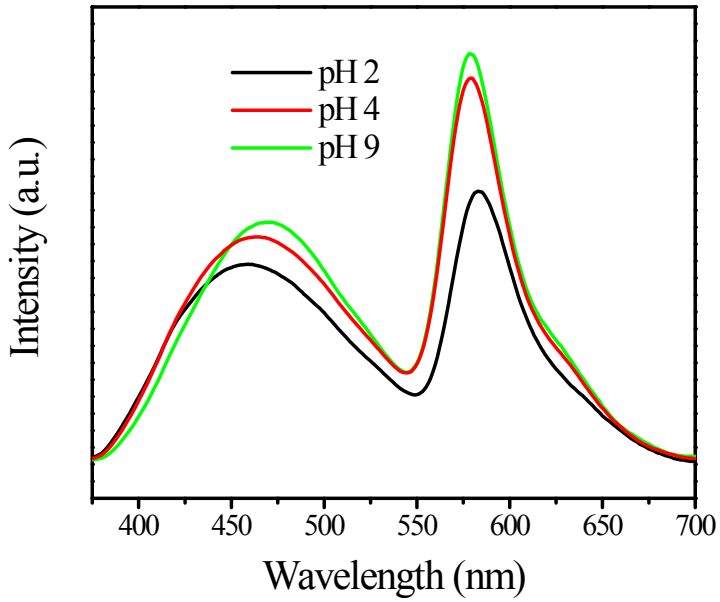

Figure S13. Variation in fluorescence intensity of C-dot-RhB composite with varying pH.

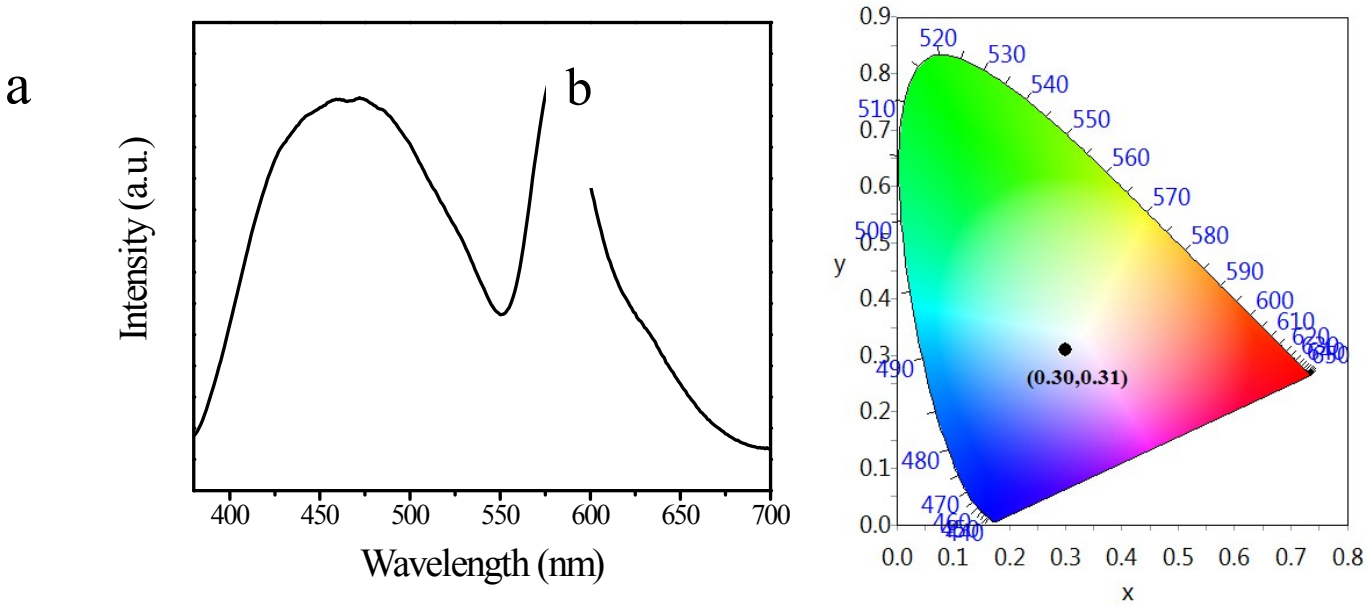

Figure S14. (a) Emission spectrum of C-dot-RhB incorporated gelatin gel and (b) Corresponding CIE plot.

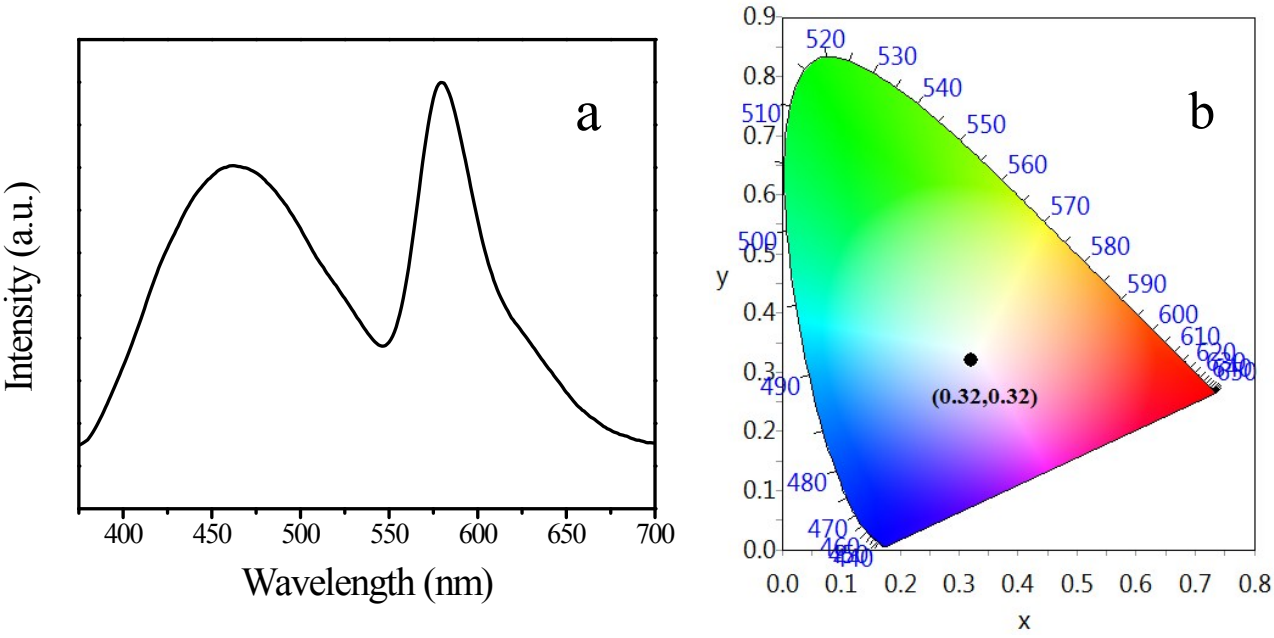

Figure S15. (a) Emission spectrum of C-dot-RhB incorporated PVA film and (b) Corresponding CIE plot.

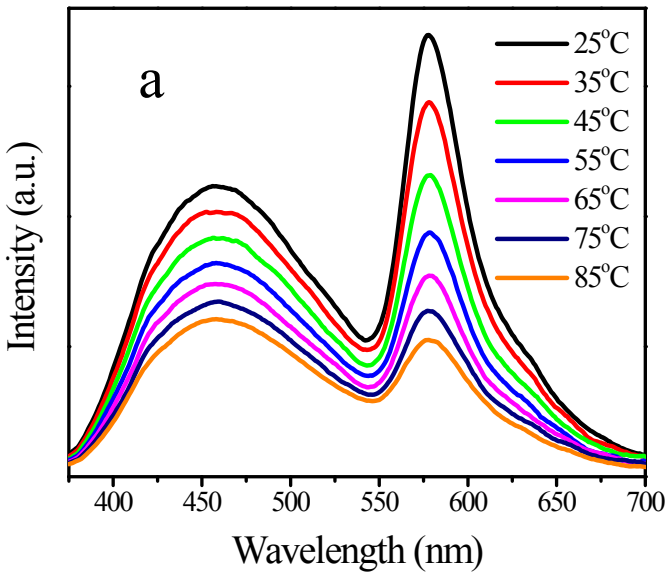

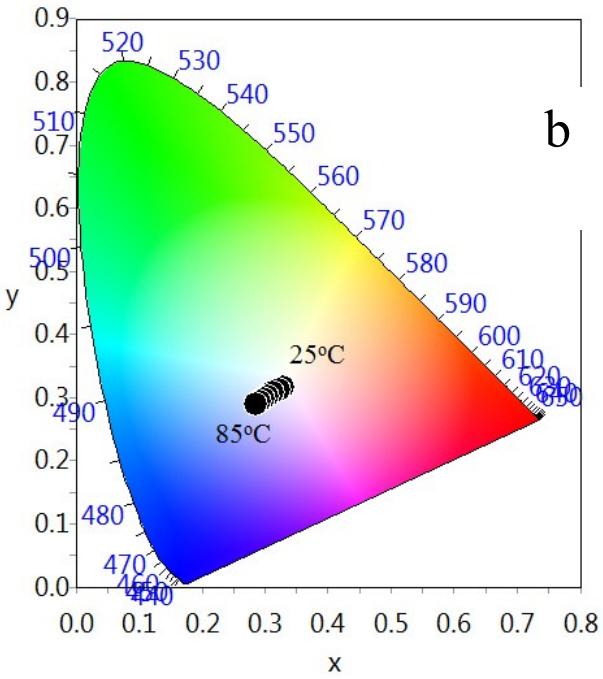

Figure S16.(a) Emission spectrum of C-dot-RhB composite at various temperatures and (b) Corresponding CIE plot.